Inorg. Chem. **2002**, *41*, 6225–6236

Models for Cytochromes *c*′: Spin States of Mono(imidazole)-Ligated (*meso*-Tetramesitylporphyrinato)iron(III) Complexes as Studied by UV−Vis, ^{13}C NMR, ^{1}H NMR, and EPR Spectroscopy

Akira Ikezaki[†] and Mikio Nakamura*[,†,‡]

Department of Chemistry, School of Medicine, Toho University, Tokyo 143-8540, Japan, and Division of Biomolecular Science, Graduate School of Science, Toho University, Funabashi 274-8510, Japan

Received June 3, 2002

A number of mono(imidazole)-ligated complexes of perchloro(*meso*-tetramesitylporphyrinato)iron(III), [Fe(TMP)L]-ClO_4, have been prepared, and their spin states have been examined by ^{1}H NMR, ^{13}C NMR, and EPR spectroscopy as well as solution magnetic moments. All the complexes examined have shown a quantum mechanical spin admixed state of high and intermediate-spin ($S = 5/2$ and 3/2) states though the contribution of the $S = 3/2$ state varies depending on the nature of axial ligands. While the complex with extremely bulky 2-*tert*-butylimidazole (2-^{t}BuIm) has exhibited an essentially pure $S = 5/2$ state, the complex with electron-deficient 4,5-dichloroimidazole (4,5-Cl_2Im) adopts an $S = 3/2$ state with 30% of the $S = 5/2$ spin admixture. On the basis of the ^{1}H and ^{13}C NMR results, we have concluded that the $S = 3/2$ contribution at ambient temperature increases according to the following order: 2-^{t}BuIm < 2-(1-EtPr)Im < 2-MeIm ≤ 2-EtIm ≤ 2-^{i}PrIm < 4,5-Cl_2Im. The effective magnetic moments determined by the Evans method in CH_2Cl_2 solution are 5.9 and 5.0 μ_B at 25 °C for [Fe(TMP)(2-^{t}BuIm)]ClO_4 and [Fe(TMP)-(2-MeIm)]ClO_4, respectively, which further verify the order given above. Comparison of the NMR and EPR data has revealed that the $S = 3/2$ contribution changes sensitively by the temperature; the $S = 3/2$ contribution decreases as the temperature is lowered for all the mono(imidazole) complexes examined in this study. The solvent polarity also affects the spin state; polar solvents such as methanol and acetonitrile increase the $S = 3/2$ contribution while nonpolar solvents such as benzene decrease it. These results are explained in terms of the structurally flexible nature of the mono(imidazole) complexes; structural parameters such as the Fe(III)–N_{axial} bond length, displacement of the iron from the N4 core, tilting of the Fe(III)–N_{axial} bond to the heme normal, orientation of the coordinated imidazole ligand, etc., could be altered by the nature of the axial ligands as well as by the solvent polarity and temperature. Some mysteries on the spin states of cytochromes *c*′ isolated from various bacterial sources are possibly explained in terms of the flexible nature of the mono(imidazole)-ligated structure.

Introduction

Cytochromes *c*′ are a unique class of heme proteins found in photosynthetic, denitrifying, and nitrogen fixing bacteria. The heme iron is pentacoordinated with a solvent-exposed histidine residue as the fifth ligand.[1] These proteins exhibit unusual EPR spectra which are ascribed to a unique spin state, a quantum mechanical admixture of a high-spin ($S = 5/2$) and an intermediate-spin ($S = 3/2$) state.[2,3] Contribution of the $S = 5/2$ or 3/2 state changes depending on the bacteria. In most cases, the oxidized form of iron is predominantly in the $S = 5/2$ spin state though the contribution of the $S = 3/2$ state increases in cytochromes *c*′ isolated from some bacteria such as *C. vinosum* and *Rb. capsulatus*.[3,4] To reveal the factors affecting the spin states of cytochromes *c*′, a systematic study using synthetic models is necessary. Several groups proposed that the model complexes such as [Fe(OEP)]ClO_4 exhibit a spin state similar to that of

* To whom correspondence should be addressed. E-mail: mnakamu@med.toho-u.ac.jp.
† Department of Chemistry, School of Medicine, Toho University.
‡ Division of Biomolecular Science, Graduate School of Science, Toho University, Funabashi 274-8510, Japan.

(1) Weber, P. C.; Bartsch, R. G.; Cusanovich, M. A.; Hamlin, R. C.; Howard, A.; Jordan, S. R.; Kamen, M. D.; Meyer, T. E.; Weatherford, D. W.; Xuong, N. h.; Salemme, F. R. *Nature* **1980**, *286*, 302−304.
(2) Maltempo, M. M. *J. Chem. Phys.* **1974**, *61*, 2540−2547.
(3) Fujii, S.; Yoshimura, T.; Kamada, H.; Yamaguchi, K.; Suzuki, S.; Shidara, S.; Takakuwa, S. *Biochim. Biophys. Acta* **1995**, *1251*, 161−169.
(4) Maltempo, M. M.; Moss, T. H.; Cusanovich, M. A. *Biochim. Biophys. Acta* **1974**, *342*, 290−305.

10.1021/ic020378t CCC: $22.00
Published on Web 10/29/2002

cytochromes *c*′.[5−12] Since then, a number of model complexes that reproduce the spin states of cytochromes *c*′ have been prepared and their spectroscopic, magnetic, and crystallographic properties have been characterized.[13−18] However, the preparation of the model complexes with the mono(imidazole) coordination has been hampered because of the instability of the mono-adducts relative to the corresponding bis-adducts.[19−23] For example, even if less than 1.0 equiv of imidazole (L) is added to a CH_2Cl_2 solution of [Fe(TPP)Cl], the bis(imidazole) adduct $[Fe(TPP)L_2]Cl$ becomes the sole product, leaving the unreacted [Fe(TPP)Cl] in solution.[24] Valentine and co-workers reported the formation of mono(imidazole) adducts such as $[Fe(TPP)(4\text{-MeIm})]SbF_6$ and characterized the complexes by means of UV−vis and EPR spectroscopy.[19] In the previous paper, we reported that the addition of less than 1.0 equiv of sterically hindered imidazoles(L's) such as 1,2-dimethylimidazole to the complex with a weak ClO_4^- ligand, $[Fe(TPP)]ClO_4$, led to the formation of the mono(imidazole) adducts $[Fe(TPP)L]ClO_4$ together with the μ-oxo dimer.[25] We have then expected that the addition of 1.0 equiv of hindered imidazoles to $[Fe(TMP)ClO_4]$ could form the corresponding mono(imidazole) adducts $[Fe(TMP)L]ClO_4$ as a sole product since the formation of the μ-oxo dimer is prohibited due to the presence of the *ortho*-methyl groups.[26] We have actually observed what we expected and have reported the NMR results of some mono(imidazole) complexes as a communication.[23] Since the method to obtain mono(imidazole) adducts in high concentration has been established, our next purpose is to reveal the factors affecting the spin states of these complexes. We have measured the UV−vis, ^{1}H NMR, ^{13}C NMR, and EPR spectra of a number of $[Fe(TMP)L]ClO_4$ as shown in Chart 1, where L's are HIm, 2-RIm (R = Me, Et, ^{i}Pr, ^{t}Bu), 1-Me-2-RIm (R = Me, Et, ^{i}Pr), some alkyl-substituted benzimidazoles, and halogenated imidazole. We have also measured the solution magnetic moments of some mono(imidazole) complexes. On the basis of the spectroscopic and magnetic results, the factors affecting the spin state of mono(imidazole) ligated complexes have been extracted. This study sheds light on the longstanding problems on the spin states of cytochromes *c*′.

Chart 1

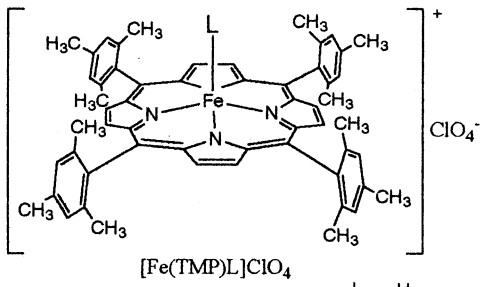

[Fe(TMP)L]ClO_4

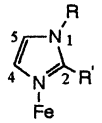

R	R′	Imidazoles
H	H	HIm
H	Me	2-MeIm
H	Et	2-EtIm
H	^{i}Pr	2-^{i}PrIm
H	^{t}Bu	2-^{t}BuIm
Me	H	1-MeIm
Me	Me	1,2-Me_2Im
Me	Et	1-Me-2-EtIm
Me	^{i}Pr	1-Me-2-^{i}PrIm

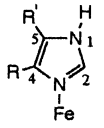

R	R′	Imidazoles
H	Me	5-MeIm
Cl	Cl	4,5-Cl_2Im

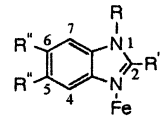

R	R′	R″	Imidazoles
H	H	H	BzIm
H	Me	H	2-MeBzIm
Me	Me	H	1,2-Me_2BzIm
H	H	Me	5,6-Me_2BzIm

Experimental Section

Materials. 2-MeBzIm, 1,2-Me_2BzIm, 5,6-Me_2BzIm, HIm, 1-MeIm, 2-MeIm, 2-EtIm, 2-^{i}PrIm, 4-MeIm, and 1,2-Me_2Im were purchased from Tokyo Kasei, and 4,5-Cl_2Im was purchased from Aldrich. These imidazoles were purified either by sublimation or by recrystallization from benzene before use. $TMPH_2$, $TMPH_2$(py-d_8), $TMPH_2$(meta-d_8), and their iron(III) chlorides and perchlorates were prepared according to the literature.[7,27]

Synthesis. (i) 2-^{t}BuIm. 2-^{t}BuIm was prepared according to the literature.[28] To a solution of pivalaldehyde (2.00 g) in methanol

(5) Dolphin, D. H.; Sams, J. R.; Tsin, T. B. *Inorg. Chem.* **1977**, *16*, 711−713.
(6) Kastner, M. E.; Scheidt, W. R.; Mashiko, T.; Reed, C. A. *J. Am. Chem. Soc.* **1978**, *100*, 666−667.
(7) Reed, C. A.; Mashiko, T.; Bentley, S. P.; Kastner, M. E.; Scheidt, W. R.; Spartalian, K.; Lang, G. *J. Am. Chem. Soc.* **1979**, *101*, 2948−2958.
(8) Ogoshi, H.; Sugimoto, H.; Yoshida, Z.-I. *Biochim. Biophys. Acta* **1980**, *621*, 19−28.
(9) Masuda, H.; Taga, T.; Osaki, K.; Sugimoto, H.; Yoshida, Z.-I.; Ogoshi, H. *Inorg. Chem.* **1980**, *19*, 950−955.
(10) Ogoshi, H.; Sugimoto, H.; Watanabe, E.-I.; Yoshida, Z.-I. Maeda, Y.; Sakai, H. *Bull. Chem. Soc. Jpn.* **1981**, *54*, 3414−3419.
(11) Boersma, A. D.; Goff, H. M. *Inorg. Chem.* **1982**, *21*, 581−586.
(12) Abbreviations: TPP, TMP, and T^{i}PrP, dianions of *meso*-tetraphenyl-, *meso*-tetramesityl-, and *meso*-tetraisopropyl-porphyrin; OEP: dianion of 2,3,7,8,12,13,17,18-octaethylporphyrin; $[Fe(TMP)]ClO_4$, perchloro(*meso*-tetramesitylporphyrinato)iron(III); 2-RIm, 2-alkylimidazole, where R is Me (methyl), Et (ethyl), ^{i}Pr (isopropyl), ^{t}Bu (*tert*-butyl); 1-Me-2-RIm, 1-methyl-2-alkylimidazole; BzIm, benzimidazole; 2-MeBzIm, 2-methylbenzimidzole; 1,2-Me_2BzIm, 1,2-dimethylbenzimidazole; 4,5-Cl_2Im, 4,5-dichloroimidazole.
(13) Toney, G. E.; Gold, A.; Savrin, J.; Ter Haar, L. W.; Sangaiah, R.; Hatfield, W. E. *Inorg. Chem.* **1984**, *23*, 4350−4352.
(14) Kintner, E. T.; Dawson, J. H. *Inorg. Chem.* **1991**, *30*, 4892−4897.
(15) Reed, C. A.; Guiset, F. *J. Am. Chem. Soc.* **1996**, *118*, 3281−3282.
(16) Ikeue, T.; Saitoh, T.; Yamaguchi, T.; Ohgo, Y.; Nakamura, M.; Takahashi, M.; Takeda, M. *Chem. Commun.* **2000**, 1989−1990.
(17) Simonato, J.-P.; Pécaut, J.; Pape, L. Le; Oddou, J.-L.; Jeandey, C.; Shang, M.; Scheidt, W. R.; Wojacyński, J.; Wołowiec, S.; Latos-Grażyński, L.; Marchon, J.-C. *Inorg. Chem.* **2000**, *39*, 3978−3987.
(18) Nesset, M. J. M.; Cai, S.; Shokhireva, T. K.; Shokhirev, N. V.; Jacobson, S. E.; Jayaraj, K.; Gold, A.; Walker, F. A. *Inorg. Chem.* **2000**, *39*, 532−540.
(19) Quinn, R.; Nappa, M.; Valentine, J. S. *J. Am. Chem. Soc.* **1982**, *104*, 2588−2595.
(20) Scheidt, W. R.; Geiger, D. K.; Lee, Y. J.; Reed, C. A.; Lang, G. *J. Am. Chem. Soc.* **1985**, *107*, 5693−5699.
(21) Gupta, G. P.; Lang, G.; Scheidt, W. R.; Geiger, D. K.; Reed, C. A., *J. Chem. Phys.* **1985**, *83*, 5945−5952.
(22) Fujii, H.; Yoshimura, T.; Kamada, H. *Inorg. Chem.* **1997**, *36*, 6142−6143.
(23) Ikezaki, A.; Nakamura, M. *Chem. Lett.* **2000**, 994−995.
(24) Walker, F. A.; Lo, M.-W.; Ree, M. T. *J. Am. Chem. Soc.* **1976**, *98*, 5552−5560.
(25) Ikezaki, A.; Nakamura, M., *J. Inorg. Biochem.* **2001**, *84*, 137−144.
(26) Groves, J. T.; Haushalter, R. C.; Nakamura, M.; Nemo, T. E.; Evans, B. J. *J. Am. Chem. Soc.* **1981**, *103*, 2884−2886.
(27) Groves, J. T.; Quinn, R.; McMurry, T. J.; Nakamura, M.; Lang, G.; Boso, B. *J. Am. Chem. Soc.* **1985**, *107*, 354−360.

(20 mL) was added 40% glyoxal (3.39 g) in 50 mL of water. The solution was cooled to 0 °C to which 28% aqueous NH_3 (11.44 g) was added. After the mixture was stirred for 15 h, the white solid precipitated was collected by filtration. The solid was dried for 1 day to yield the crude product, which was purified by sublimation. Yield: 1.15 g (40%). ^{1}H NMR (25 °C, δ): 1.35 (9H, s, CH_3), 6.91 (2H, s, ring CH), 8.99 (1H, s, NH).

(ii) 2-(1-EtPr)Im. This compound was similarly prepared from 2-ethylbutanal, glyoxal, and NH_3. Yield: 1.33 g (41%). ^{1}H NMR (25 °C, δ): 0.81 (6H, t, CH_3), 1.70 (4H, m, CH_2), 2.61 (1H, m, CH), 6.95 (2H, s, ring CH), 10.18 (1H, s, NH). ^{13}C NMR (25 °C, δ): 12.1 (CH_3), 27.9 (CH_2), 43.6 (CH), 121.6 (4,5-C), 152.0 (2-C).

Spectral Measurements. For UV−vis measurements, a CH_2Cl_2 solution of [Fe(TMP)]ClO_4 was prepared in a graduated flask and used as a standard solution. A constant volume of the solution was taken from the standard solution and poured into several 5 mL graduated flasks containing various amounts of 2-MeIm. The concentration of [Fe(TMP)]ClO_4 for the UV−vis measurement was maintained at 7.7 μM by the addition of a certain volume of CH_2Cl_2. The UV−vis spectra were measured on a SHIMADZU MultiSpec-1500 spectrophotometer at ambient temperature. For ^{1}H NMR measurement, a 7.5 mM CD_2Cl_2 standard solution of [Fe(TMP)]ClO_4 was prepared. In each measurement, a 550 μL CD_2Cl_2 solution was taken from the standard solution and poured into an NMR sample tube under argon atmosphere. A CD_2Cl_2 standard solution of imidazole was prepared so that 20 μL corresponds to 1.0 equiv relative to [Fe(TMP)]ClO_4. After the addition of the relevant imidazole, the ^{1}H NMR spectra were taken on a JEOL LA300 spectrometer operating at 300.4 MHz for ^{1}H. Chemical shifts were referenced to the residual peaks of CD_2Cl_2, δ = 5.32 ppm. For ^{13}C NMR measurements, a CD_2Cl_2 solution containing 20 mg of [Fe(TMP)]ClO_4 was placed in an NMR sample tube, to which a CD_2Cl_2 solution containing 1.0−1.5 equiv of imidazole was added with a microsyringe to form a ca. 40 mM solution. The ^{13}C NMR spectra were taken on a JEOL LA300 spectrometer. Chemical shifts were referenced to the residual peaks of CD_2Cl_2, δ = 53.8 ppm. For EPR measurement, a 80 μL CH_2Cl_2 solution was taken from the 7.5 mM stock solution and placed into an EPR sample tube. After the addition of 1.0−1.5 equiv of imidazole, the EPR spectra were recorded at 4.2 K on a Brucker E500 spectrometer operating at X band and equipped with an Oxford helium cryostat.

Effective Magnetic Moments. The effective magnetic moments (μ_1^{eff}) were determined in solution by the Evans method using CH_2Cl_2 as the chemical shift reference.[29] The magnetic moments (μ_1^{eff}) of the reaction products were determined relative to that of high-spin [Fe(TMP)Cl] (μ_2^{eff} = 5.92 μ_B) according to $\mu_1^{eff} = (\Delta\nu_1/\Delta\nu_2)^{1/2}\mu_2^{eff}$, where $\Delta\nu_1$ and $\Delta\nu_2$ are the difference in chemical shifts of CH_2Cl_2 in [Fe(TMP)L]ClO_4 and [Fe(TMP)Cl], respectively.

Results and Discussion

Formation of Mono-Adducts [Fe(TMP)L]ClO_4. (1) UV−Vis Spectroscopy. Figure 1a shows the UV−vis spectral change observed when 2-MeIm was added up to 1.25 equiv relative to [Fe(TMP)]ClO_4. As the ligand was added, the intensity of the Soret band of [Fe(TMP)]ClO_4 at 398 nm weakend and a new band at 412 nm increased with isosbestic points at 370 and 407 nm. Similar spectral change was observed in the Q-band regions. The new complex shows λ_{max} (log ϵ) at 412 (4.99), 511 (4.05), 572 (3.46), and 692 (3.41) nm. Figure 1b shows the UV−vis spectral change observed when a much larger amount of 2-MeIm, 1.25−15 000 equiv, was added to the solution. The Soret band at 412 nm showed a red shift with increased intensity and reached 418 nm. The complex obtained by the addition of 15 000 equiv of 2-MeIm is easily identified as the bis-adduct [Fe(TMP)(2-MeIm)$_2$]ClO_4 by the spectral comparison with the authentic sample. Thus, the complex formed by the addition of 1.25 equiv of 2-MeIm is assigned to the mono-addcut [Fe(TMP)(2-MeIm)]ClO_4. Table 1 shows the λ_{max} values of a series of [Fe(TMP)L]ClO_4 together with those of the corresponding bis-adducts. The λ_{max} values of the

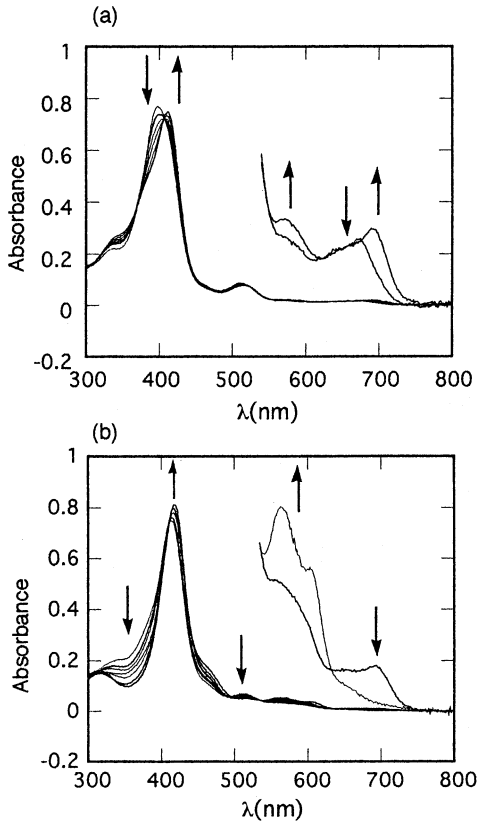

Figure 1. (a) UV−vis spectral change obtained by the addition of 0−1.25 equiv of 2-MeIm to a CH_2Cl_2 solution of [Fe(TMP)]ClO_4 at ambient temperature. The blue and red lines correspond to the UV−vis spectra of [Fe(TMP)]ClO_4 and [Fe(TMP)(2-MeIm)]ClO_4, respectively. (b) UV−vis spectral change obtained by the addition of 1.25−15 000 equiv of 2-MeIm to a CH_2Cl_2 solution of [Fe(TMP)]ClO_4 at ambient temperature.

Table 1. UV−Vis Absorption Maxima (λ_{max}, nm) of [Fe(TMP)L]ClO_4 and [Fe(TMP)L_2]ClO_4 Determined at 25 °C in CH_2Cl_2 Solution

L	[Fe(TMP)L]ClO_4				[Fe(TMP)L_2]ClO_4				
Him	412	510	575	690	416	453(sh)		551	
2-MeIm	412	511	572	692	418	459(sh)	515	563	600
2-EtIm	412	513	570	693	419	460(sh)	520	563	602
2-^{i}PrIm	414	510	571	689	418	463(sh)	516	562	602
2-(1-EtPr)Im	413	510	579	692	a				
2-^{t}BuIm	414	509	561	691	a				

[a] Formation of the bis-adducts is not observed even by the addition of 2000 equiv of the ligands.

(28) Matsuura, T.; Ikari, M. *Kogyo Kagaku Zasshi* **1969**, *72*, 179−183 (in Japanese).
(29) Evans, D. F.; James, T. A. *J. Chem. Soc.* **1979**, 723−726.

Table 2. ^{1}NMR Chemical Shifts (δ, ppm) of [Fe(TMP)L]ClO_4 Determined by 25 °C in CD_2Cl_2 Solution Together with Int(%)[a]

axial ligands	pyrrole	meta	Int(%)
HIm	20.7 (15.1)	13.2, 12.5 (16.9, 15.5)	42
5-MeIm	31.0 (40.4)	13.7, 12.8 (18.1, 16.4)	35
2-MeIm	35.1 (29.3)	14.3, 13.2 (17.5, 15.6)	32
2-EtIm	32.4 (16.9)	14.1, 13.1 (16.7, 15.0)	34
2-^{i}PrIm	30.5 (4.4)	14.0, 13.1 (15.9, 14.5)	35
2-(1-EtPr)Im	54.1 (84.4)	15.4, 14.1 (20.2, 17.5)	19
2-^{t}BuIm	78.5 (122.6)	13.0, 12.0 (17.2, 15.1)	1
1,2-Me_2Im	25.4 (29.6)	13.9, 12.9 (17.8, 15.9)	39
1-Me-2-EtIm	19.0 (−12.0)	13.4, 12.6 (14.9, 13.6)	44
1-Me-2-^{i}PrIm	13.9 (−23.5)	13.2, 12.4 (14.1, 13.0)	47
BzIm	27.7 (28.4)	14.0, 13.0 (18.2, 16.1)	37
5,6-Me_2BzIm	43.3 (70.1)	14.9, 13.6 (19.2, 16.8)	26
2-MeBzIm	27.0 (−13.4)	14.1, 13.0 (14.8, 13.2)	38
1,2-Me_2BzIm	13.7[b] (−26.6)	13.5, 12.5[b] (14.1, 12.7)	47
4,5-Cl_2Im	−15.3[b] (−56.2)	10.5, 10.5[b] (12.4, 11.6)	68
Cl^- [c]	79.8 (125.2)	15.9, 14.3 (22.2, 19.2)	0
ClO_4^- [d]	−9.3 (−61.6)	11.4 (11.6)	64

[a] Data in parentheses are the chemical shifts at −80 °C. [b] Data are obtained by the extrapolation from low temperature. [c] [Fe(TMP)Cl]. [d] [Fe(TMP)]ClO_4.

monoadducts are quite close to those reported by Valentine et al. for [Fe(TPP)(4-MeIm)]SbF_6 in toluene solution.[19]

(2) ^{1}H NMR Spectroscopy. Formation of the mono(imidazole) adducts is also confirmed by the ^{1}H NMR spectral change observed when imidazoles are added to the CD_2Cl_2 solutions of [Fe(TMP)]ClO_4. Table 2 lists the chemical shifts of a series of mono(imidazole) adducts assigned on the basis of the discussion given below.

(i) Imidazole (HIm) Adduct. Figure 2 shows the ^{1}H NMR spectra observed after the addition of imidazole (HIm) to the CD_2Cl_2 solution of [Fe(TMP)]ClO_4. When 0.29 equiv of HIm relative to [Fe(TMP)]ClO_4 was added, each signal corresponding to [Fe(TMP)]ClO_4 decreased in intensity and the new signals assigned to the pyrrole (20.7 ppm) and *meta* protons (12.5 and 13.2 ppm) increased; the assignment of these signals was unambiguously done by the spectral comparison with the deuterated complexes. Three signals with equal integral intensities appeared fairly downfield, 48.0, 84.3, and 99.6 ppm. These signals were assigned to the ring protons of the coordinated imidazole. Since the integral intensity of each signal was 1/8 of that of the pyrrole signal at 20.7 ppm, the product was identified as the mono(imidazole) adduct [Fe(TMP)(HIm)]ClO_4. When 0.87 equiv of HIm was added, the signals for [Fe(TMP)]ClO_4 further decreased in intensity and those for the well-characterized bis(imidazole) adduct [Fe(TMP)$(HIm)_2$]ClO_4 appeared. The population ratios of [Fe(TMP)]ClO_4, [Fe(TMP)(HIm)]ClO_4, and [Fe(TMP)$(HIm)_2$]ClO_4 were estimated to be 24, 67, and 9%, respectively. The rate of ligand dissociation in the monoadduct is slow on the ^{1}H NMR time scale at 25 °C because the pyrrole and *meta* signals of the three complexes appeared separately. Further addition of imidazole increased the bis-adduct, which became a sole component when 2.2 equiv of the ligand was added.

(ii) 5,6-Dimethylbenzimidazole (5,6-Me_2BzIm) Adduct. Figure 3 shows the ^{1}H NMR spectral change observed when 5,6-dimethylbenzimidazole (5,6-Me_2BzIm) was added to the CD_2Cl_2 solution of [Fe(TMP)]ClO_4. By the addition of 1.25 equiv of the ligand, the signals for [Fe(TMP)]ClO_4 almost disappeared. In contrast to the case of HIm, the signals for the bis(imidazole) adduct were not observable. Thus, the solution contains almost exclusively the mono-adduct [Fe(TMP)(5,6-Me_2BzIm)]ClO_4, which shows the pyrrole signal at 43.3 and *meta* signals at 13.6 and 14.9 ppm. Two methyl signals of the coordinated imidazole, each corresponding to 3H relative to the pyrrole signal, were observed at 8.2 and −0.2 ppm. A broad signal corresponding to 1H appeared at fairly downfield, 52.2 ppm, which was assigned to one of the ring protons of the coordinated ligand. When more than 1.25 equiv of the ligand was added, every signal started to broaden, suggesting that the ligand exchange occurs on the ^{1}H NMR time scale between the mono- and bis-adducts; the rate for ligand exchange is much faster in [Fe(TMP)(5,6-Me_2BzIm)]ClO_4 than in [Fe(TMP)(Im)]ClO_4 due to the steric bulkiness of 5,6-Me_2BzIm. By the addition of 3.0 equiv of the ligand, a broad pyrrole signal for the bis-adduct was observed at −6.7 ppm.

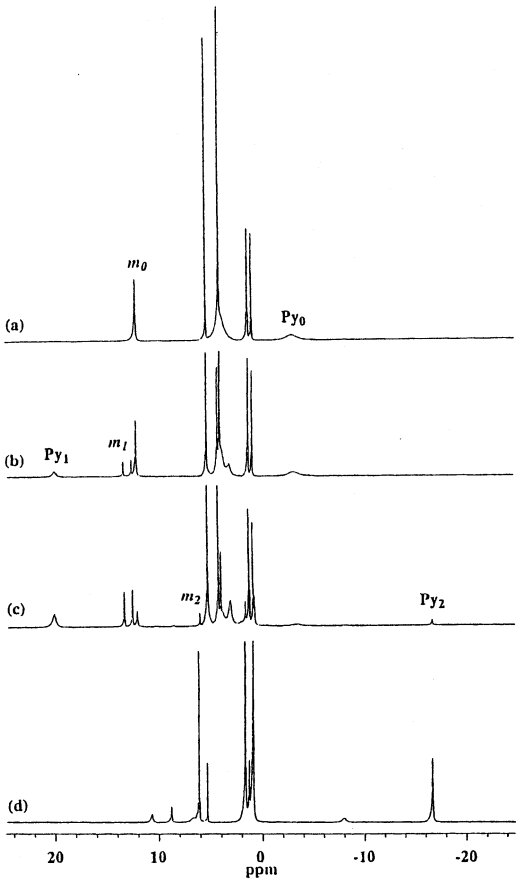

Figure 2. ^{1}H NMR spectral change of [Fe(TMP)]ClO_4 taken in CD_2Cl_2 solution at 25 °C after the addition of various amounts of HIm: (a) 0.0 equiv; (b) 0.29 equiv; (c) 0.87 equiv; (d) 2.3 equiv. Signals labeled by m_0, m_1, and m_2 and Py_0, Py_1, and Py_2 are the *meta* and pyrrole protons of [Fe(TMP)]ClO_4, [Fe(TMP)(HIm)]ClO_4, and [Fe(TMP)$(HIm)_2$]ClO_4, respectively.

(iii) 2-*tert*-Butylimidazole (2-^{t}BuIm) Adduct. Figure 4a shows the ^{1}H NMR spectrum of the sample prepared by the addition of 1.5 equiv of 2-^{t}BuIm into the CD_2Cl_2 solution of [Fe(TMP)]ClO_4. Formation of the mono(imidazole) adduct is clearly shown by the *tert*-butyl signal at −1.38 ppm together with the two *meta* signals at 12.0 and 13.0 ppm.

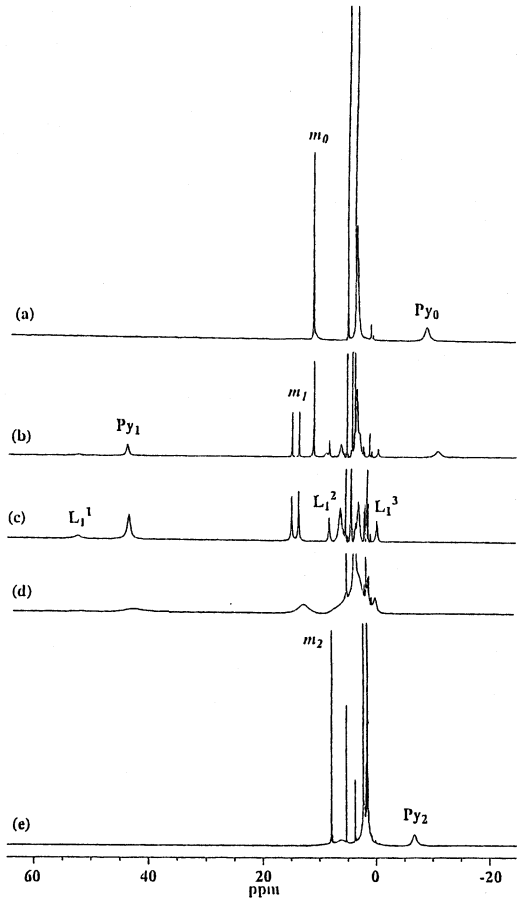

Figure 3. ^{1}H NMR spectral change of [Fe(TMP)]ClO_4 taken in CD_2Cl_2 solution at 25 °C after the addition of various amount of 5,6-Me_2BzIm: (a) 0.0 equiv; (b) 0.50 equiv; (c) 1.25 equiv: (d) 1.5 equiv; (e) 3.0 equiv. L_1^1 is assigned to one of the ring protons, and L_1^2 and L_1^3 are due to the methyl protons of the axial ligand in [Fe(TMP)(5,6-Me_2BzIm)]ClO_4.

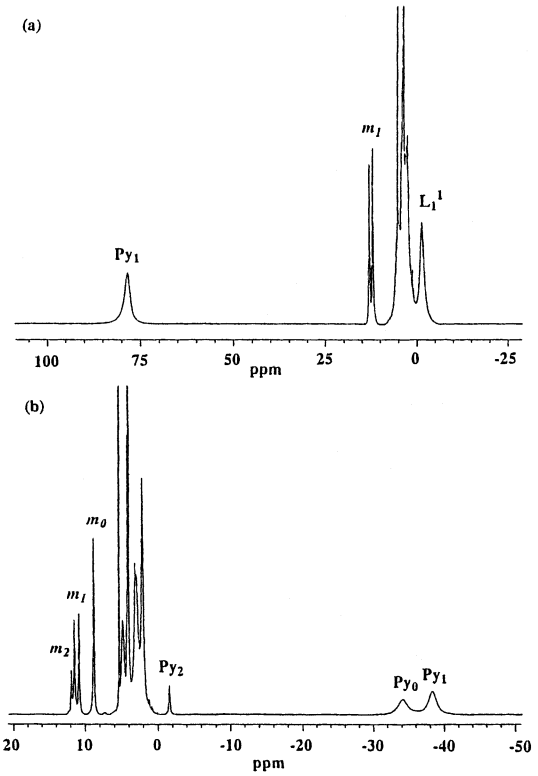

Figure 4. (a) ^{1}H NMR spectrum of [Fe(TMP)(2-^{t}BuIm)]ClO_4 obtained by the addition of 1.5 equiv of 2-^{t}BuIm into a CD_2Cl_2 solution of [Fe(TMP)]ClO_4 at 25 °C. (b) ^{1}H NMR spectrum of [Fe(TMP)(4,5-Cl_2Im)]ClO_4 obtained by the addition of 1.0 equiv of 4,5-Cl_2Im into a CD_2Cl_2 solution of [Fe(TMP)]ClO_4 at −50 °C.

The pyrrole signal appeared fairly downfied, 78.5 ppm. By further addition of the ligand, the *tert*-butyl signal gradually moved downfield, indicating that the interconversion between the coordinated and free ligands occurs rapidly. Even by the addition of large excess of the ligand, the bis-adduct was not formed since no appreciable spectral change was observed for the pyrrole and *meta* signals.

(iv) 4,5-Dichloroimidazole (4,5-Cl_2Im) Adduct. The pyrrole signal of [Fe(TMP)]ClO_4 moved upfield as the ligand was added at 25 °C. After the addition of 1.0 equiv of the ligand, the pyrrole signal shifted to −17.5 ppm; the *meta* signal showed little change and appeared at 10.6 ppm as a singlet. Thus, the NMR spectrum is quite similar to that of [Fe(TMP)]ClO_4 except for the position of the pyrrole signals. The result suggests that the ligand exchange among three possible species, [Fe(TMP)]ClO_4, [Fe(TMP)(4,5-Cl_2Im)]ClO_4, and [Fe(TMP)(4,5-Cl_2Im)$_2$]ClO_4, is fast on the ^{1}H NMR time scale. To freeze the ligand exchange process, the ^{1}H NMR spectra were measured at lower temperature. Both the pyrrole and *meta* signals broadened and started to split below 0 °C. At −50 °C, clearly separated signals were observed at −34.1, −38.3, and −1.6 ppm for the pyrrole protons as shown in Figure 4b. The signal at −34.1 ppm was assigned to the pyrrole protons of [Fe(TMP)]ClO_4 on the basis of the spectral comparison with the authentic sample. By the addition of an excess amount of the ligand, the signal at −1.6 ppm increased in intensity and those at −34.1 and −38.3 ppm decreased. Thus, the signals at −38.3 and −1.6 ppm were assigned to the pyrrole protons of the mono- and bis-adducts, respectively. The *meta* signals for the three complexes are similarly assigned; two signals at 10.8 and 11.5 ppm were assigned to the *meta* signals of the mono-adduct. The small signal was observed fairly downfield, 114.1 ppm, which was assigned to the coordinated imidazole proton of the mono-adduct since the integral intensity of this signal is ca. 1/8 of that of the pyrrole signal at −38.3 ppm.

(v) Mono-Adduct of Other Imidazoles. Mono-adducts of a wide variety of imidazoles were similarly prepared. In general, hindered imidazoles such as 2-alkylimidazoles, 1-methyl-2-alkylimidazoles, and benzimidazoles tend to form rather pure mono-adducts by the addition of 1.1−1.3 equiv of the ligands. Quite pure mono(imidazole) adducts was obtained in solution when excess amount of the extremely bulky 2-(1-EtPr)Im was added. In contrast, the contamination of the bis-adduct was observed when less hindered imidazoles such as HIm and 1-MeIm were added.

Reasons for the Formation of Mono(imidazole) Adducts. Bis(imidazole) adducts are usually prepared by the addition of more than 2.0 equiv of imidazoles to the solutions of (porphyrinato)iron(III) chlorides. Thus, a possible procedure to prepare a mono(imidazole) adduct is to add exactly 1.0 equiv of the imidazole ligand. However, mono(imidazole) adducts are difficult to obtain by this method, because the

K_1 value for eq 1 is much smaller than the K_2 value for eq 2 when X is a commonly used chloride ligand; K_1 and K_2 values are reported to be 1.6×10^1 and 3.3×10^3 M^{-1}, respectively, for the formation of [Fe(TPP)(2-MeIm)]Cl and [Fe(TPP)(2-MeIm)$_2$]Cl.[24]

$$[\text{Fe(porphyrin)X}] + \text{L} \rightleftarrows [\text{Fe(porphyrin)L}]\text{X} \quad (1)$$

$$[\text{Fe(porphyrin)L}]\text{X} + \text{L} \rightleftarrows [\text{Fe(porphyrin)L}_2]\text{X} \quad (2)$$

In the present study, we used [Fe(TMP)]ClO_4 instead of [Fe(TMP)Cl]. Because of a fairly weak ligand field strength of ClO_4^-,[15,30] a quantitative reaction took place in most cases; addition of 1.0 equiv of imidazoles led to the exclusive formation of mono(imidazole) adducts. The result indicates that K_1 of [Fe(TMP)]ClO_4 is much larger than that of [Fe(TPP)Cl]. In fact, the K_1 value for the formation of [Fe(TMP)(2-MeIm)]ClO_4 was estimated graphically from the change in absorbance at 397 nm to be 2.1×10^6 M^{-1} according to the method of Rossotti and Rossotti.[31−33] Thus, the K_1 value of [Fe(TMP)]ClO_4 toward 2-MeIm increased 1.3×10^5 times as much as that of [Fe(TPP)Cl]! The large K_1 value should be ascribed to the weak Fe(III)−ClO_4 bond as compared with the Fe(III)−Cl bond. Several lines of evidence on the weak Fe(III)−ClO_4 bonding have been obtained by the NMR spectroscopy. For example, [Fe(TMP)Cl] showed two signals for the *meta* protons in CD_2Cl_2 solution, while only one signal was observed for [Fe(TMP)]ClO_4. The result suggests that the ligand dissociation takes place rapidly in the latter complex, which in turn indicates the weak Fe(III)−ClO_4 bonding in CD_2Cl_2 solution. In C_6D_6 solution, however, the *meta* protons of [Fe(TMP)]ClO_4 showed two signals, suggesting that the Fe(III)−ClO_4 bond is strengthened in a less polar C_6D_6 solution. Correspondingly, a considerable amount of the bis-adduct was formed in C_6D_6 solution even in the reaction between [Fe(TMP)]ClO_4 and 1.0 equiv of 2-MeIm; the solution contained 20 and 30% of the mono- and bis-adducts, respectively, together with [Fe(TMP)]ClO_4. The high preference of Cl^- toward Fe(III) was also clearly exhibited by the following experiment: addition of 0.5 equiv of $Bu_4N^+Cl^-$ into the CD_2Cl_2 solution of [Fe(TMP)(2-MeIm)]ClO_4 almost quantitatively decomposed the mono-adduct to give [Fe(TMP)(2-MeIm)$_2$]ClO_4 and [Fe(TMP)Cl] according to eq 3.

$$2[\text{Fe(TMP)(2-MeIm)}]ClO_4 + Bu_4N^+Cl^- \rightleftarrows [\text{Fe(TMP)Cl}] + [\text{Fe(TMP)(2-MeIm)}_2]ClO_4 + Bu_4N^+ClO_4^- \quad (3)$$

Steric effects also contribute greatly to the formation of the mono(imidazole) adducts. In this study, we used [Fe(TMP)]ClO_4 instead of [Fe(TPP)]ClO_4. Because of the presence of the bulky *ortho*-methyl groups, formation of the bis-adduct could be hampered due to the strong steric repulsion between the axial ligand and *ortho*-methyl groups. In fact, the K_2 value of [Fe(TMP)(2-MeIm)$_2$]ClO_4, 4.8×10^4 M^{-1}, is much smaller than that of [Fe(TPP)(4-MeIm)$_2$]SbF_6, 10^7 M^{-1}, reported by Valentine and co-workers.[19] Thus, in the case of extremely bulky 2-^{t}BuIm, only the mono-adduct was formed even in the presence of excess amount of the ligand.

Spin States of Mono(imidazole) Adducts. Spin states of mono(imidazole) adducts have been examined on the basis of the ^{1}H NMR, ^{13}C NMR, and EPR spectroscopic results as well as magnetic measurement.

(1) ^{1}H NMR. (i) Chemical Shifts of the Pyrrole Protons. Chemical shifts of the pyrrole protons and their temperature dependence are good probes to determine the spin state of iron(III) ions.[34−36] In the case of high-spin ($S = 5/2$) complexes, the β-pyrrole protons give signals fairly downfield, ca. 80 ppm at 25 °C. These signals move further downfield as the temperature is lowered. In the case of intermediate-spin ($S = 3/2$) complexes, the unpaired electrons in the d_{xz} and d_{yz} orbitals are transferred to the porphyrin ring via $3e_g$(porphyrin)−d_π(iron) orbital interactions. Since the $3e_g$ orbitals have large coefficients at the pyrrole β-carbons, the interactions induce considerable amount of spin densities on these carbon atoms. Thus, the pyrrole signals of the protons directly bonded to these carbons appear at extremely upfield position and move further upfield as the temperature is lowered; the purest intermediate-spin complex, [Fe(TPP)]($CB_{11}H_6Cl_6$), shows the pyrrole signal at −62 ppm at 25 °C.[15] In the case of the admixed intermediate-spin ($S = 3/2, 5/2$) complexes, the pyrrole signals appear between these two extremes, +80 to −60 ppm at 25 °C. The contribution of the $S = 3/2$ in the admixed $S = 5/2, 3/2$ spin system, which is signified as Int(%) in the following discussion, can be estimated on the basis of the pyrrole proton chemical shifts. If we assume that the population of the $S = 1/2$ spin state is negligibly small in the mono(imidazole) adducts, the Int(%) is given as follows, where δ is the observed chemical shift of the pyrrole protons:

$$\text{Int}(\%) = [(80 - \delta)/140] \times 100\ (\%) \quad (4)$$

It should be noted that eq 4 is applicable only to the iron(III) complexes of *meso*-tetraarylpoprhyrins such as TPP and TMP; pure intermediate-spin complexes with highly ruffled porphyrin ring such as [Fe(T^{i}PrP)(THF)$_2$]ClO_4 show pyrrole signals at much more downfield region due to the less effective overlaps between the iron d_π and porphyrin $3e_g$ orbitals.[16,37] The Int(%) values of a series of mono(imidazole)

(30) Evans, D. R.; Reed, C. A. *J. Am. Chem. Soc.* **2000**, *122*, 4660−4667.
(31) Rossotti, F. J. C.; Rossotti, H. In *The Determination of Stability Constants*; McGraw-Hill: New York, 1961; p 277.
(32) Neya, S. Morishima, I.; Yonezawa, T. *Biochemistry* **1981**, *20*, 2610−2614.
(33) Scheidt, W. R.; Lee, Y. J.; Luangdilok, W.; Haller, K. J.; Anzai, K.; Hatano, K. *Inorg. Chem.* **1983**, *22*, 1516−1522.
(34) Goff, H. In *Iron Porphyrins*; Lever, A. B. P., Gray, H. B., Eds.; Physical Bioinorganic Chemistry Series 1; Addison-Wesley: Reading, MA, 1983; Part I, pp 237−281.
(35) Walker, F. A.; Simonis, U. *Paramagnetic Molecules*; Berliner, L. J., Reuben, J., Eds.; Biological Magnetic Resonance, Vol. 12; Plenum Press: New York, 1993; pp 133−274.
(36) Walker, F. A. In *The Porphyrin Handbook*; Kadish, K. M., Smith, K. M., Guilard, R., Eds.; Academic Press: San Diego, CA, 2000; Vol. 5, Chapter 36, pp 81−183.
(37) Bertini, I.; Luchinat, C. In *NMR of Paramagnetic Substances*; Lever, A. B. P., Ed.; Coordination Chemistry Reviews 150; Elsevier: Amsterdam, 1996; pp 29−75.

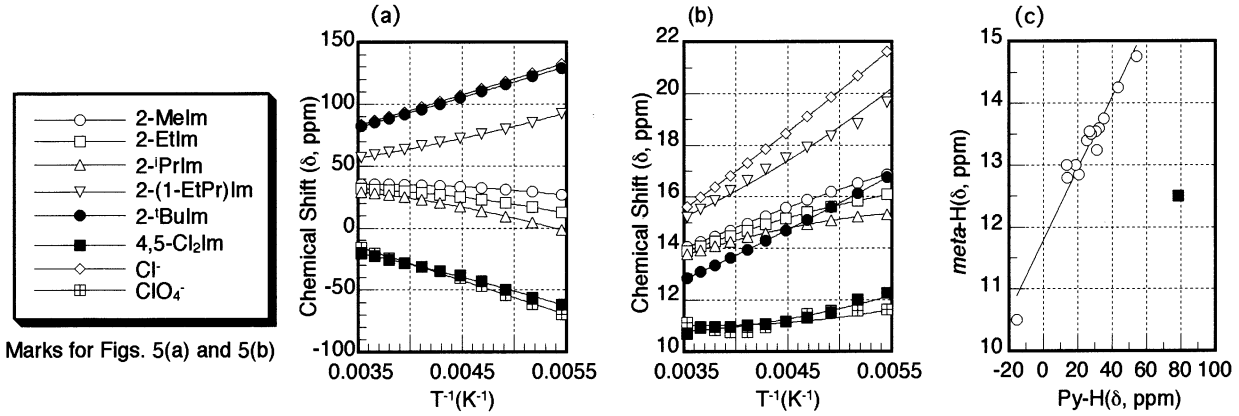

Figure 5. Curie plots of the pyrrole and *meta* proton signals of some mono(imidazole) complexes: (a) pyrrole signals; (b) averaged *meta* signals; (c) correlation of the chemical shifts between the pyrrole and *meta* proton signals. [Fe(TMP)(2-^{t}BuIm)]ClO_4 is given by ■.

complexes at 25 °C are listed in Table 2. It is worth describing that the Int(%) values are quite different between [Fe(TMP)(2-^{i}PrIm)]ClO_4 and [Fe(TMP)(2-^{t}BuIm)]ClO_4, 35 and 1%, respectively, though both complexes carry bulky imidazole ligands. Thus, [Fe(TMP)(2-^{t}BuIm)]ClO_4 exhibits an essentially pure high-spin character. In contrast, [Fe(TMP)(4,5-Cl_2Im)]ClO_4 has a quite large Int(%), ca. 70%, as is revealed from the existence of a fairly upfield shifted pyrrole signal, −15.3 ppm at 25 °C. On the basis of the chemical shifts listed in Table 2 and the Curie plots shown in Figure 5a, we have concluded that the Int(%) increases according to the order given by eq 5.

$$2\text{-}^t\text{BuIm} < 2\text{-(1-EtPr)Im} < 2\text{-MeIm} \leq 2\text{-EtIm} \leq 2\text{-}^i\text{PrIm} < 4,5\text{-}Cl_2\text{Im} \quad (5)$$

(ii) Chemical Shifts of the *meta*-Phenyl Protons. One of the characteristic features in the ^{1}H NMR spectra of high-spin complexes such as [Fe(TPP)Cl] and [Fe(TMP)Cl] is the downfield shift of the *meta*-phenyl protons; [Fe(TMP)Cl] gives these signals at 14.3 and 15.9 ppm at 25 °C.[34−36] The pure intermediate-spin complex [Fe(TPP)]($CB_{11}H_6Cl_6$) shows the corresponding signals at 9.1 ppm in benzene solution.[15] Thus, the chemical shift of the *meta*-phenyl protons can also be a probe to determine the spin states. Although the difference in chemical shifts of the two extremes is rather small, 5−7 ppm, the chemical shifts in Table 2 and the Curie plots given in Figure 5b roughly correspond to eq 5 determined by the pyrrole shifts. A notable exception is [Fe(TMP)(2-^{t}BuIm)]ClO_4 which shows the *meta* signals much more upfield than they are expected from the chemical shifts of the pyrrole protons. Figure 5c shows the correlation between the pyrrole shifts and the averaged *meta* shifts of the 15 mono-adducts. Good linear line with correlation coefficient of 0.973 has been observed if we exclude the data of [Fe(TMP)(2-^{t}BuIm)]ClO_4. In the case of [Fe(TMP)(2-^{t}BuIm)]ClO_4, the *meso* mesityl groups and the coordinated 2-^{t}BuIm ligand are supposed to rotate about the $C_{meso}-C_{ipso}$ and Fe(III)$-N_{axial}$ bonds, respectively, to remove the severe steric repulsion, which could induce the upfield shift of the *meta* signal.

(iii) Chemical Shifts of the Ligand Protons. The chemical shifts of the ligand protons are listed in Table S1 of the Supporting Information. All the complexes examined show the ring protons at fairly downfield region, 48−120 ppm. The results suggest that the complex has unpaired electron in the d_{z^2} orbital, which is transferred to the ligand protons through σ bonds to induce downfield shift. Since both the high-spin and intermediate-spin complexes have unpaired electron in the d_{z^2} orbital, it must be difficult to extract the information on the spin states on the basis of the chemical shifts of the ligand protons.

Table 3. ^{13}C NMR Chemical Shifts (δ, ppm) of Carbons in [Fe(TMP)L]ClO_4 Determined at 25 °C in CD_2Cl_2 Solution

axial ligands	α-Py	β-Py	meso	ortho
HIm	637	748	305	274, 259
5-MeIm	774	855	322	290, 273
2-MeIm	755	888	393	314, 302
2-EtIm	717	862	391	311, 299
2-^{i}PrIm	679	836	390	308, 297
2-(1-EtPr)Im	1051	1147	448	351, 342
2-^{t}BuIm	1294	1343	368	322, 302
1,2-Me_2Im	643	800	375	300, 290
1-Me-2-EtIm	545	727	368	291, 282
1-Me-2-^{i}PrIm	446	654	368	285, 276
BzIm	670	809	349	293, 281
5,6-Me_2BzIm	914	1002	381	320, 306
2-MeBzIm	549	775	437	316, 309
1,2-Me_2BzIm	383	645	413	241, 216
Cl^- [a]	1204	1327	525	408, 372
ClO_4^- [b]	176	377	252	217

[a] [Fe(TMP)Cl]. [b] [Fe(TMP)]ClO_4.

(2) ^{13}C NMR. We have established that ^{13}C NMR spectroscopy is a powerful tool for determining the spin state and electron configurations of iron(III).[38−42] Table 3 lists the chemical shifts of some carbon atoms. In the case of the high-spin complexes, the unpaired electron in the $d_{x^2-y^2}$ orbital is transferred to the porphyrin carbons via σ bonds. Thus, these carbons give signals at fairly downfield; the chemical shifts of the α-pyrrole, β-pyrrole, and *meso* carbons

(38) Ikeue, T.; Ohgo, Y.; Saitoh, T.; Nakamura, M.; Fujii, H.; Yokoyama, M. *J. Am. Chem. Soc.* **2000**, *122*, 4068−4076.
(39) Ikeue, T.; Ohgo, Y.; Saitoh, T.; Yamaguchi, T.; Nakamura, M. *Inorg. Chem.* **2001**, *40*, 3423−3434.
(40) Ikeue, T.; Ohgo, Y.; Yamaguchi, T.; Takahashi, M.; Takeda, M.; Nakamura, M. *Angew. Chem., Int. Ed.* **2001**, *40*, 2617−2620.
(41) Ikezaki, A.; Nakamura, M. *Inorg Chem.* **2002**, *41*, 2761−2768.
(42) Ikezaki, A.; Ikeue, T.; Nakamura, M. *Inorg. Chim. Acta* **2002**, *335*, 91−99.

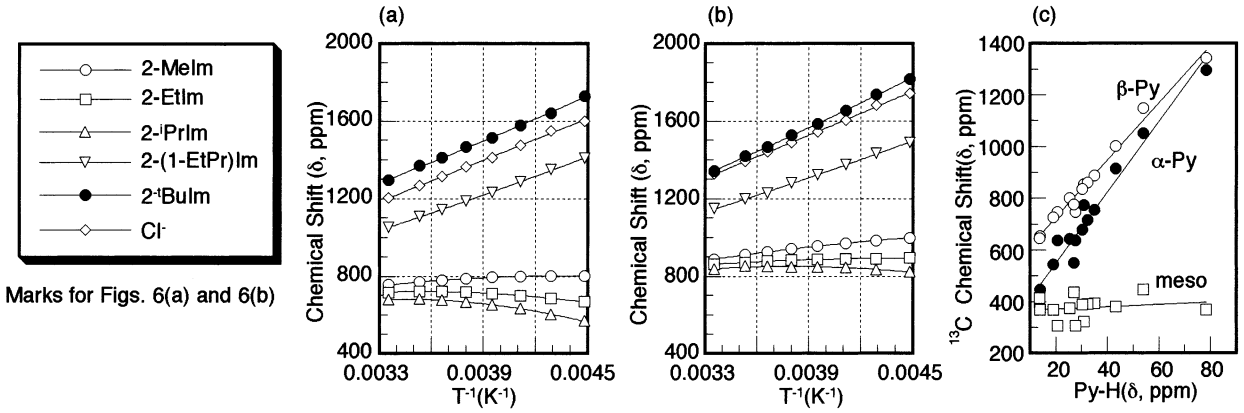

Figure 6. Curie plots of the carbon signals of mono(imidazole) complexes: (a) α-pyrrole signals; (b) *β*-pyrrole signals; (c) correlation of the chemical shifts of the α-pyrrole, *β*-pyrrole, and *meso* carbons against the chemical shifts of the pyrrole protons.

at 25 °C are 1204, 1327, and 525 ppm, respectively, in [Fe(TMP)Cl]. In the case of the intermediate-spin complexes, these carbons should give signals at much more upfield region because of the absence of unpaired electron in the $d_{x^2-y^2}$ orbital. Thus, the increase in the upfield shifts of the porphyrin carbons corresponds to the increase in the $S = 3/2$ contribution. Figure 6a,b shows the Curie plots of the α- and *β*-pyrrole carbon signals of a series of [Fe(TMP)L]ClO_4, respectively. The upfield shifts of the α- and *β*-pyrrole signals clearly increase by the same order given in eq 5. Figure 6c shows the correlation of the chemical shifts of the pyrrole protons with those of the α-pyrrole, *β*-pyrrole, and *meso* carbons in all the mono(imidazole) adducts examined in this study. Good linearity with correlation coefficients of 0.981 and 0.990 is observed for the α- and *β*-pyrrole carbons, respectively. The correlation is, however, quite poor for the *meso* carbons, suggesting that the chemical shifts of the *meso* carbons are not much different between the $S = 5/2$ and $S = 3/2$ spin states. Thus, the *meso* carbon shifts cannot be a good probe to determine the contribution of the $S = 3/2$ in the admixed $S = 5/2$, 3/2 spin system.

(3) EPR. EPR spectra were taken for the complexes obtained by the addition of 1.0−1.3 equiv of a series of imidazole ligands (L's) to CH_2Cl_2 solutions of [Fe(TMP)]ClO_4. Figure 7 shows some typical spectra obtained by the addition of (a) L = HIm, (b) 5-MeIm, (c) 2-MeBzIm, and (d) 2-*t*BuIm. The EPR spectra commonly showed a small signal at $g = 4.3$ ascribed to the starting [Fe(TMP)]ClO_4, except for those of the complexes carrying sterically very hindered imidazoles such as 2-*t*BuIm. Figure 7a shows some intense signals around $g = 2.8$ and 2.3 in addition to the signal at $g = 4.3$. The spectrum indicates that the mono(imidazole) adduct [Fe(TMP)(HIm)]ClO_4, which is the major species at the temperature range where the NMR spectra are taken, decomposed to [Fe(TMP)]ClO_4 and [Fe(TMP)$(HIm)_2$]ClO_4 according to eq 6; [Fe(TMP)$(HIm)_2$]ClO_4 is reported to show a rhombic EPR spectrum with $g = 2.92$, 2.29, and 1.57.[43]

$$2[\mathrm{Fe(TMP)(HIm)}]\mathrm{ClO_4} \leftrightarrows [\mathrm{Fe(TMP)(HIm)_2}]\mathrm{ClO_4} + [\mathrm{Fe(TMP)}]\mathrm{ClO_4} \quad (6)$$

Figure 7b also shows weak rhombic signals at $g = 2.9$ and 2.3 ascribed to the bis-adduct [Fe(TMP)(5-MeIm)$_2$]ClO_4. Figure 7c shows an axial signal at $g = 2.53$ ascribed to [Fe(TMP)(2-MeBzIm)$_2$]ClO_4.[44] The axial type EPR spectrum indicates that the complex has low-spin iron(III) with the less common $(d_{xz}, d_{yz})^4(d_{xy})^1$ electron configuration.[35,36,38,39] As mentioned, Figure 7d shows a quite pure spectrum for the mono-adduct; no signals for the bis-adduct nor for [Fe(TMP)]ClO_4 were observed. Table 4 lists the g values determined by the computer simulation of the observed spectra. The Int(%) values, calculated by $100(6 - g_\perp)/2$ in the admixed $S = 5/2$, 3/2 spin system, are also listed in Table 4.[45] As the data in Table 4 indicate, most of the complexes have shown similar degree of spin admixture, 8−10%. Some mono(imidazole) complexes carrying less hindered imidazoles such as Him and 5-MeIm exhibit slightly larger Int(%) values. In contrast, the mono(imidazole) complexes with sterically very hindered imidazoles such as 2-(1-EtPr)Im and

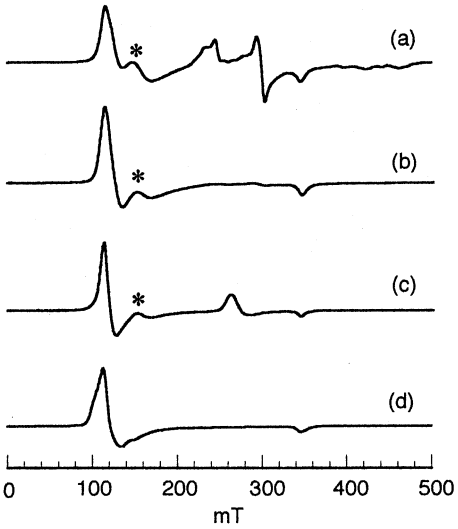

Figure 7. EPR spectra (CH_2Cl_2, 4.2 K) of the samples obtained by the addition of 1.1−1.3 equiv of imidazoles into [Fe(TMP)]ClO_4, where imidazoles are (a) HIm, (b) 5-MeIm, (c) 2-MeBzIm, and (d) 2-*t*BuIm. The signal for [Fe(TMP)]ClO_4 is signified by the asterisk.

(43) Nakamura, M.; Tajima, K.; Tada, K.; Ishizu, K.; Nakamura, N. *Inorg. Chim. Acta* **1994**, *224*, 113−124.
(44) Nakamura, M.; Nakamura, N. *Chem. Lett.* **1991**, 1885−1888.
(45) Palmer, G. In *Iron Porphyrins*; Lever, A. B. P., Gray, H. B., Eds.; Addison Wesley: Reading, MA, 1982; Part II, pp 43−88.

Table 4. EPR *g* Values of a Series of Mono(imidazole) Complexes Taken in Frozen CH_2Cl_2 Solution at 4.2 K

axial ligands	g_x	g_x	g_x	Int(%)
HIm	5.75	5.65	1.99	15
5-MeIm	5.80	5.60	1.99	15
2-MeIm	5.90	5.70	2.00	10
2-EtIm	5.90	5.70	1.99	10
2-^{i}PrIm	5.90	5.70	1.99	10
2-(1-EtPr)Im	6.00	5.80	1.99	5
2-^{t}BuIm	6.25	5.75	1.99	0
1-Me-2-EtIm	5.85	5.70	2.00	11
1-Me-2-^{i}PrIm	6.10	5.70	2.00	10
BzIm	5.90	5.60	2.00	13
5,6-Me_2BzIm	6.00	5.60	1.99	10
2-MeBzIm	5.90	5.80	1.99	8
1,2-Me_2BzIm	5.95	5.75	2.00	8

2-^{t}BuIm have shown much smaller spin admixture; the 2-^{t}BuIm complex exhibits an essentially pure high-spin state. Several discrepancies exist among the data obtained by the EPR and NMR methods; while the ^{1}H and ^{13}C NMR methods have revealed that both [Fe(TMP)(1-Me-2-^{i}PrIm)]ClO_4 and [Fe(TMP)(1,2-Me_2BzIm)]ClO_4 show 47% of the $S = 3/2$ contribution, the EPR method exhibits only 8−10%. The discrepancies should be ascribed to the difference in temperatures where the spectra are taken; EPR spectra were taken at 4.2 K while NMR spectra were measured at 170−300 K. Comparison of the data in Tables 2 and 4 reveals that the Int(%) values at 298 K are larger than those at 4.2 K for all the complexes examined. The results could be explained in terms of the temperature dependence of the structural change. In the previous paper, we reported that the Fe(III)−N_{axial} bonds in six-coordinated [Fe(OETPP)Py_2]ClO_4 specifically contract as the temperature is lowered.[46] Since the contraction of the Fe(III)−N_{axial} bond corresponds to the increase in the axial ligand field, it destabilizes the d_{z^2} orbital and increases the $S = 5/2$ contribution in the $S = 5/2$, 3/2 admixed spin system.[47]

(4) Effective Magnetic Moments. Determination of the effective magnetic moments of mono-adducts is difficult because of the contamination of a small amount of bis-adduct and/or starting [Fe(TMP)]ClO_4 complex. Thus, the effective magnetic moments were measured by the Evans method only for the mono-adducts carrying bulky imidazoles such as [Fe(TMP)(2-MeIm)]ClO_4, [Fe(TMP)(5,6-Me_2BzIm)]ClO_4, and [Fe(TMP)(2-^{t}BuIm)]ClO_4; these complexes can be obtained without appreciable contamination of the other complexes as is revealed from the ^{1}H NMR spectra shown in Figures 3 and 4a. The effective magnetic moments of [Fe(TMP)(2-MeIm)]ClO_4, [Fe(TMP)(5,6-Me_2BzIm)]ClO_4, and [Fe(TMP)-(2-^{t}BuIm)]ClO_4 were determined to be 5.0, 5.2, and 5.9 μ_B, respectively, at 25 °C in CH_2Cl_2 solution. Thus, the results are consistent with the order given in eq 4.

Factors Affecting the Spin States of Mono(imidazole) Adducts. (i) Steric Effects of Imidazole. As mentioned, this study has shown that the Int(%) is influenced by the bulkiness of the 2-R group in a series of [Fe(TMP)(2-RIm)]ClO_4. Extremely bulky imidazoles such as 2-^{t}BuIm and 2-(1-EtPr)-Im exhibit smaller Int(%) as compared with less bulky imidazoles such as 2-MeIm, 2-EtIm, and 2-^{i}PrIm; the Int-(%) is nearly 0% in the case of 2-^{t}BuIm complex. Extensive works on the admixed $S = 5/2$, 3/2 spin state in five-coordinate iron(III) porphyrins have revealed that the Int-(%) increases if either one or some of the following conditions are satisfied: (i) The axial ligand field is weakened.[15] (ii) The deviation of iron from the N4 plane is decreased.[48] (iii) Electron-donating groups are introduced at the porphyrin periphery.[13,18] (iv) The porphyrin ring is deformed.[49,50] The steric repulsion between the 2-R group and the porphyrin core in [Fe(TMP)(2-RIm)]ClO_4 could expand the distance between the imidazole nitrogen and the N4 plane; the Fe−N_{axial} bond length increases form 1.975 to 2.004 Å as the axially coordinated 1-MeIm is replaced by 2-MeIm in low-spin six-coordinated $[Fe(TMP)L_2]^+$.[51,52] In the case of [Fe(TMP)(2-^{t}BuIm)]ClO_4, the distance should be the largest because of the severe steric repulsion between the *tert*-butyl group and the porphyrin core. As a result, the central iron is dragged toward the imidazole nitrogen and is located at the position where the deviation from the N4 plane is larger than that in any other complexes. Increase in the out-of-plane deviation of iron should stabilize the $S = 5/2$ spin state because the energy level of the $d_{x^2-y^2}$ orbital drops. The deviation of iron is expected to be smaller as the axial ligand changes from bulky 2-^{t}BuIm to less bulky 2-MeIm, 2-EtIm, and 2-^{i}PrIm, resulting in the increase in the Int(%) of the corresponding complexes. It is difficult, however, to explain the subtle increase in the Int(%) values on going from [Fe(TMP)(2-MeIm)]ClO_4 to [Fe(TMP)(2-EtIm)]ClO_4 and then to [Fe(TMP)(2-^{i}PrIm)]ClO_4; the chemical shift of the pyrrole signal changes from 29.3 to 16.9 and then to 4.4 ppm at −80 °C. Similar tendency is found in a series of [Fe(TMP)(1-Me-2-RIm)]ClO_4 as is clearly shown in the ^{1}H and ^{13}C NMR chemical shifts listed in Tables 2 and 3; the chemical shifts of the pyrrole protons are 29.6, −12.0, and −23.5 ppm at −80 °C for R = Me, Et, and ^{i}Pr, respectively. The coordination structures of these complexes such as the Fe(III)−N_{axial} bond length, the out-of-plane displacement of the Fe(III) ion from the N4 plane, the tilting of the Fe(III)−N_{axial} bond from the heme normal, and the orientation of the imidazole plane relative to the diagonal $N_{pyrrole}$−Fe−$N_{pyrrole}$ axes could mainly be determined by the steric interactions of the axial ligand with the porphyrin core and/or *meso* mesityl groups; the electronic effects are supposed to be quite similar among 2-alkylimidazoles. Because the R groups are either primary or secondary, the steric repulsion between the axial ligand and the porphyrin core is not much different among the complexes; the steric repulsion could be relieved

(46) Ohgo, Y.; Ikeue, T.; Nakamura, M. *Inorg. Chem.* **2002**, *41*, 1698−1700.
(47) Weber, P. C. *Biochemistry* **1982**, *21*, 5116−5119.
(48) Scheidt, W. R. In *The Porphyrin Handbook*; Kadish, K. M., Smith, K. M., Guilard, R., Eds.; Academic Press: San Diego, CA, 2000; Vol. 3, Chapter 16, pp 49−112.
(49) Nakamura, M.; Ikeue, T.; Ohgo, Y.; Takahashi, M.; Takeda, M. *Chem. Commun*. **2002**, 1198−1199.
(50) Barkigia, K. M.; Renner, M. W.; Fajer, J. J. *Porphyrins Phthalocyanines* **2001**, *5*, 415−418.
(51) Scheidt, W. R.; Kirner, J. F.; Hoard, J. L.; Reed, C. A. *J. Am. Chem. Soc*. **1987**, *109*, 1963−1968.
(52) Safo, M. K.; Gupta, G. P.; Walker, F. A.; Scheidt, W. R. *J. Am. Chem. Soc*. **1991**, *113*, 5497−5510.

by the conformational change of the alkyl group. On the other hand, the steric repulsion between the axial ligand and the *meso* mesityl groups must be different depending on the bulkiness of the alkyl group. Scheidt and co-workers recently reported that the off-axis tilt of the Fe(II)−N_{axial} bond from the normal to the porphyrin ring in [Fe(TPP)(2-MeIm)] is 8.3°.[53] The off-axis tilt must be much larger in [Fe(TMP)(2-^{i}PrIm)]$^+$ due to the presence of the *ortho*-methyl groups and much bulkier 2-isopropyl group. As a result, the tilt angle in [Fe(TMP)(2-^{i}PrIm)]$^+$ is expected to be larger than those in [Fe(TMP)(2-EtIm)]$^+$ and [Fe(TMP)(2-MeIm)]$^+$, which in turn weakens the ligand field strength of the 2-^{i}PrIm ligand. Thus, the out-of-plane displacement of the iron decreases in [Fe(TMP)(2-^{i}PrIm)]$^+$, leading to the increase in the $S = 3/2$ contribution. To compare the ligand field strength between the 2-MeIm and 2-^{i}PrIm ligands in the mono(imidazole) complexes, the NMR samples consisting of [Fe(TMP)]ClO_4 and 0.5 equiv of the ligands were prepared. The ^{1}H NMR spectra of these samples showed 1:1 mixture of [Fe(TMP)]ClO_4 and [Fe(TMP)L]ClO_4. As the temperature is raised, the *meta* and pyrrole signals started to broaden due to the ligand exchange. While the half-height width of the *meta* signal increased from 13 Hz at 25 °C to 178 Hz at 80 °C in [Fe(TMP)(2-^{i}PrIm)]ClO_4, the corresponding signal in [Fe(TMP)(2-MeIm)]ClO_4 showed much smaller increase, 15 Hz at 25 °C and 44 Hz at 80 °C. The results suggest that the 2-^{i}PrIm ligand in [Fe(TMP)(2-^{i}PrIm)]ClO_4 is more labile than the 2-MeIm ligand in [Fe(TMP)(2-MeIm)]ClO_4, which in turn suggests that the ligand field strength of the 2-^{i}PrIm ligand is much weaker than that of the 2-MeIm ligand in the mono(imidazole) complexes [Fe(TMP)L]ClO_4. Detailed comparison of the molecular structures of [Fe(TMP)(2-^{t}BuIm)]ClO_4, [Fe(TMP)(2-^{i}PrIm)]ClO_4, and [Fe(TMP)(2-MeIm)]ClO_4 determined by the X-ray crystallographic analyses are necessary to prove the speculation, which is now in progress in this laboratory; only one example has been reported on the structural analysis of 5-coordinate mono(imidazole) complex, [Fe(OEP)(2-MeIm)]$^+$.[20]

(ii) Electronic Effects of Imidazole. NMR and EPR results have shown that the contribution of the $S = 3/2$ in the admixed $S = 5/2$, 3/2 spin system varies from an essentially pure $S = 5/2$ state to the predominant $S = 3/2$ state depending on the nature of the axially coordinated imidazole ligands. Obviously, the electron-withdrawing substituents at the imidazole ring are playing an important role to stabilize the $S = 3/2$ spin state as is revealed from the pyrrole proton chemical shifts of [Fe(TMP)(4,5-Cl_2Im)]ClO_4; the Int(%) of this complex is estimated to be 68%. Because of the presence of the electron-withdrawing groups, the ligand field strength of the imidazole is weakened and the d_{z^2} orbital is stabilized. Weak axial ligand field would also affect the deviation of iron from the mean N4 plane; the iron would be dragged toward the center of the N4 cavity by the relatively stronger equatorial ligand field as compared with the axial ligand field. Decrease in the out-of-plane deviation of iron would destabilize the $d_{x^2-y^2}$ orbital. Thus, the energy gap between the d_{z^2} and $d_{x^2-y^2}$ orbitals increases, resulting in the stabilization of the $S = 3/2$ spin state.

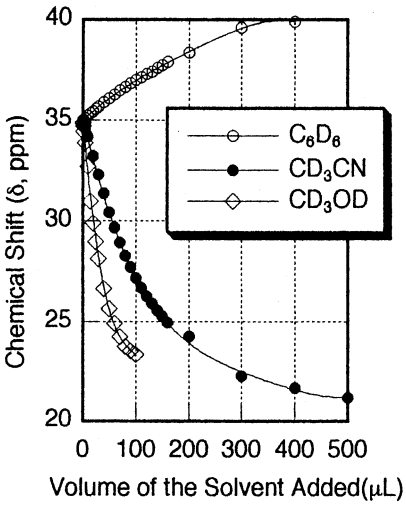

Figure 8. Change in chemical shifts of the pyrrole protons observed by the addition of various amounts of C_6D_6, CD_3CN, or CD_3OD into a CD_2Cl_2 solution of [Fe(TMP)(2-MeIm)]ClO_4 at 25 °C.

(iii) Solvent Effects. The chemical shifts of the pyrrole protons in [Fe(TMP)(2-MeIm)]ClO_4 were affected by the solvents. While the pyrrole signal was observed at 35.0 ppm in CD_2Cl_2 solution, it moved upfield as a polar solvent such as CD_3CN or CD_3OD was added to the CD_2Cl_2 solution of [Fe(TMP)(2-MeIm)]ClO_4; the pyrrole signals reached 27.2 and 23.4 ppm in CD_2Cl_2 solutions containing 15% CD_3CN and 15% CD_3OD, respectively. In contrast, the pyrrole signal moved downfield and appeared at 37.0 ppm in CD_2Cl_2 solutions containing 15% of nonpolar C_6D_6. Figure 8 shows the change in chemical shifts of the pyrrole signals observed by the addition of (a) C_6D_6, (b) CD_3CN, and (c) CD_3OD. As mentioned, the chemical shift of the pyrrole protons is a good probe to determine the $S = 3/2$ contribution. The upfield shift of the pyrrole signals in polar solvents corresponds to the increase in the Int(%). The result indicates that the Fe(III)−N_{axial} bond is weakened as the polarity of solvent increases. In other words, 2-MeIm ligand behaves as a weaker ligand in polar solvent than in less polar solvent. Thus, the Fe(III) ion is dragged toward the center of the N4 cavity, resulting in the increase in the Int(%). In nonpolar solvents such as benzene, the Fe(III)−N_{axial} bond is strengthened, resulting in the decrease in the Int(%).

Biological Implication. The oxidized cytochromes *c*′ have been studied widely by various methods such as NMR,[54−63]

(53) Ellison, M. K.; Schultz, C. E.; Scheidt, W. R. *Inorg. Chem.* **2002**, *41*, 2173−2181.

(54) Emptage, M. H.; Xavier, A. V.; Wood, J. M.; Alsaadi, B. M.; Moore, G. R.; Pitt, R. C.; Williams, R. J. P.; Ambler, R. P.; Bartsch, R. G. *Biochemistry* **1981**, *20*, 58−64.

(55) Jackson, J. T.; La Mar, G. N.; Bartsch, R. G. *J. Biol. Chem.* **1983**, *258*, 1799−1805.

(56) Akutsu, H.; Kyogoku, Y.; Horio, T. *Biochemistry* **1983**, *22*, 2055−2061.

(57) La Mar, G. N.; Jackson, J. T.; Dugad, L. B.; Cusanovich, M. A.; Bartsch, R. G. *J. Biol. Chem.* **1990**, *265*, 16173−16180.

(58) Banci, L.; Bertini, I.; Turano, P.; Vicens Oliver, M. *Eur. J. Biochem.* **1992**, *204*, 107−112.

(59) Bertini, I.; Gori, G.; Luchinat, C.; Vila, A. J. *Biochemistry* **1993**, *32*, 776−783.

(60) Caffrey, M.; Simorre, J.-P.; Brutscher, B.; Cusanovich, M.; Marion, D. *Biochemistry* **1995**, *34*, 5904−5912.

EPR,[2,3,64,65] resonance Raman,[66−69] MCD,[70] Mössbauer,[71−73] and EXAFS spectroscopy.[74] Interestingly, the contribution of the $S = 3/2$ state is different not only depending on the bacterial source of the proteins but also depending on the spectroscopic methods applied for the measurement. For example, while EPR spectroscopy has revealed that the cytochromes *c′* isolated from photosynthetic bacteria such as *Rb. capsulatus* and *R. palustris* exhibit ca. 40% of the $S = 3/2$ contribution at pH 7.2, those isolated from *R. molischianum* and *R. rubrum* have shown 13% of the $S = 3/2$ contribution.[3] Furthermore, NMR study has revealed that the latter proteins are essentially in a pure high-spin $S = 5/2$ state.[57]

Cytochromes *c′* are usually found as dimers. Despite low homology in the amino acid sequences, the overall folding of the monomers is similar. They possess a heme prosthetic group covalently bound to the protein via two thioether linkages that are provided by a conserved Cys−X−Y−Cys−His motif near the C-terminal region.[75−82] The heme iron is five-coordinated with a solvent-exposed histidine residue. Although the X-ray crystallographic analyses have revealed the structural similarity among these proteins, the microenvironment around the heme center is slightly different among the proteins. Thus, the solvent-exposed histidine residue could involve in the hydrogen bonding with water molecules and/or basic protein residues in a slightly different way among the proteins.[69,75−82] Such a difference in microenvironment is expected to alter the spin state of the Fe(III) ion. In this study, we have shown experimentally that the $S = 3/2$ contribution increases as the polar solvents such as methanol and acetonitrile are added. It is expected that the NH of the coordinated imidazole ligand involves in hydrogen bonding with polar solvents such as methanol. If this is the case, the hydrogen bonding would increase the $S = 3/2$ contribution. In fact, the X-ray crystallographic analysis of *Rb. capsulatus* has shown a hydrogen bonding between the coordinated imidazole (His122) and water molecule.[79] Correspondingly, the $S = 3/2$ contribution of the cytochrome *c′* reached as much as 40%.[3,83] In contrast, the structural analysis of *R. molischianum* has shown that the coordinated imidazole (His122) is not involved in hydrogen bonding.[75] Correspondingly, the $S = 3/2$ contribution decreased to 13% as determined by EPR spectgroscopy;[3] the $S = 3/2$ contribution was estimated as 0% by ^{1}H NMR spectroscopy.[57] On the basis of these results, we propose that *the hydrogen bonding of solvent molecules to the coordinated histidyl imidazole ligand rather weakens the ligand field strength and increases the $S = 3/2$ contribution in the admixed $S = 5/2$, 3/2 spin system*.

As mentioned, another ambiguity frequently encountered in cytochromes *c′* is that even the same species exhibits a different spin state depending on the spectroscopic methods applied for the measurement. For example, while EXAFS or EPR spectroscopy indicates a significant contribution of the $S = 3/2$ state for *R. molischianum*[3,74] or *R. rubrum*,[3,74] NMR and MCD studies suggest that these species exhibit an essentially pure $S = 5/2$ character at room temperature.[57,70] As mentioned, we have experienced similar discrepancies on the spin states in this study; the $S = 3/2$ contribution determined by the NMR method at ambient temperature is different from that determined by the EPR method at 4.2 K. The discrepancies seem to be originated from the lability intrinsic to the mono(imidazole) structure. That is, the structural parameters such as the Fe(III)−N_{axial} bond length, out-of-plane displacement of the Fe(III) ion from the N4 plane, tilting of the Fe(III)−N_{axial} bond from the heme normal, and orientation of the imidazole plane relative to the diagonal $N_{pyrrole}$−Fe−$N_{pyrrole}$ axes are easily perturbed not only by the steric and electronic effects caused by the axial ligands but by the solvent and temperature effects; lowering the temperature or changing the solvent polarity could affect the structural parameters mentioned above and induce the change in spin state of the Fe(III) ion. We have reported in the previous papers that some six-coordinated iron(III) porphyrin complexes exhibit a contraction of the Fe(III)−N_{axial} bonds as the temperature is lowered and induce the spin transition from $S = 3/2$ to $S = 1/2$.[40,46] Thus, one of the reasons for the ambiguities on the spin states of cytochromes *c′* should be ascribed to the structural change

(61) Caffrey, M.; Simorre, J.-P.; Cusanovich, M.; Marion, D. *FEBS Lett.* **1995**, *368*, 519−522.
(62) Clark, K.; Dugad, L. B.; Bartsch, R. G.; Cusanovich, M. A.; La Mar, G. N. *J. Am. Chem. Soc.* **1996**, *118*, 4654−4664.
(63) Tsan, P.; Caffrey, M.; Daku, M. L.; Cusanovich, M.; Marion, D.; Gans, P. *J. Am. Chem. Soc.* **2001**, *123*, 2231−2242.
(64) Yoshimura, T.; Suzuki, S.; Nakahara, A.; Iwasaki, H.; Masuko, M.; Matsubara, T. *Biochim. Biophys. Acta* **1985**, *831*, 267−274.
(65) Zahn, J. A.; Arciero, D. M.; Hooper, A. B.; Dispirito, A. A. *Eur. J. Biochem.* **1996**, *240*, 684−691.
(66) Strekas, T. C.; Spiro, T. G. *Biochim. Biophys. Acta* **1974**, *351*, 237−245.
(67) Kitagawa, T.; Ozaki, Y.; Kyogoku, Y.; Horio, T. *Biochim. Biophys. Acta* **1977**, *495*, 1−11.
(68) Hobbs, J. D.; Larsen, R. W.; Meyer, T. E.; Hazzard, J. H.; Cusanovich, M. A.; Ondrias, M. R. *Biochemistry* **1990**, *29*, 4166−4174.
(69) Othman, S.; Richaud, P.; Verméglio, A.; Desbois, A. *Biochemistry* **1996**, *35*, 9224−9234.
(70) Rawlings, J.; Stephens, P. J.; Nafie, L. A.; Kamen, M. D. *Biochemistry* **1977**, *16*, 1725−1729.
(71) Moss, T. H.; Bearden, A. J.; Bartsch, R. G.; Cusanovich, M. A. *Biochemistry* **1968**, *7*, 1583−1590.
(72) Emptage, M. H.; Zimmermann, R.; Que, L., Jr.; Münck, E.; Hamilton, W. D.; Orme- Johnson, W. H. *Biochim. Biophys. Acta* **1977**, *495*, 12−23.
(73) Maltempo, M. M.; Moss, T. H.; Spartalian, K. *J. Chem. Phys*. **1980**, *73*, 2100−2106.
(74) Korszun, Z. R.; Bunker, G.; Khalid, S.; Scheidt, W. R.; Cusanovich, M. A.; Meyer, T. E. *Biochemistry* **1989**, *28*, 1513−1517.
(75) Finzel, B. C.; Weber, P. C.; Hardman, K. D.; Salemme, F. R. *J. Mol. Biol*. **1985**, *186*, 627−643.
(76) Yasui, M.; Harada, S.; Kai, Y.; Kasai, N.; Kusunoki, M.; Matsuura, Y. *J. Biochem. (Tokyo)* **1992**, *111*, 317−324.
(77) Ren, Z.; Meyer, T.; McRee, D. E. *J. Mol. Biol*. **1993**, *234*, 433−445.
(78) Tahirov, T. H.; Misaki, S.; Meyer, T. E.; Cusanovich, M. A.; Higuchi, Y.; Yasuoka, N. *Nat. Struct. Biol.* **1996**, *3*, 459−464.
(79) Tahirov, T. H.; Misaki, S.; Meyer, T. E.; Cusanovich, M. A.; Higuchi, Y.; Yasuoka, N. *J. Mol. Biol.* **1996**, *259*, 467−479.
(80) Dobbs, A. J.; Anderson, B. F.; Faber, H. R.; Baker, E. N. *Acta Crystallogr., Sect. D* **1996**, *52*, 356−368.
(81) Archer, M.; Banci, L.; Dikaya, E.; Romao, M. J. *J. Biol. Inorg. Chem*. **1997**, *2*, 611−622.
(82) Shibata, N.; Iba, S.; Misaki, S.; Meyer, T. E.; Bartsch, R. G.; Cusanovich, M. A.; Morimoto, Y.; Higuchi, Y.; Yasuoka, N. *J. Mol. Biol*. **1998**, *284*, 751−760.
(83) Monkara, F.; Bingham, S. J.; Kadir, F. H. A.; McEwan, A. G.; Thomson, A. J.; Thurgood, A. G. P.; Moore, G. R. *Biochim. Biophys. Acta* **1992**, *1100*, 184−188.

around the heme center caused by the temperature where the spectral measurements are carried out.

Acknowledgment. The authors thank Dr. Takahisa Ikeue of Toho University School of Medicine for the EPR measurements. This work was supported by the Grant in Aid (No. 12020257) for Scientific Research on Priority Areas-(to M.N.) from the Ministry of Education, Culture, Sports, Science, and Technology of Japan and by the Nukada Fund for the Advancement of Science (to A.I.) of Toho University. Thanks are due to the Research Center for Molecular Materials, Institute for Molecular Science (IMS).

Supporting Information Available: Curie plots of the pyrrole-H signals of all the mono(imidazole) complexes examined in this study, Curie plots of the *meso*-, α-pyrrole, and *β*-pyrrole carbon signals, and a table of the chemical shifts of the ligand protons. This material is available free of charge via Internet at http://pubs.acs.org.

IC020378T